

Quenching of the Efficiency Droop in Cubic Phase InGaAIN Light-Emitting Diodes

Journal:	<i>Transactions on Electron Devices</i>
Manuscript ID	TED-2022-03-0579-R.R1
Manuscript Type:	Regular
Date Submitted by the Author:	06-Apr-2022
Complete List of Authors:	Tsai, Yi-Chia; University of Illinois at Urbana-Champaign, Electrical and Computer Engineering Leburton, Jean-Pierre; University of Illinois at Urbana-Champaign, Department of Electrical and Computer Engineering Bayram, Can; University of Illinois at Urbana-Champaign, Department of Electrical and Computer Engineering
Area of Expertise:	Light-emitting diodes, Gallium compounds, Semiconductor device modeling

SCHOLARONE™
Manuscripts

Quenching of the Efficiency Droop in Cubic Phase InGaAlN Light-Emitting Diodes

Yi-Chia Tsai, Jean-Pierre Leburton, *Life Fellow, IEEE*,
and Can Bayram, *Senior Member, IEEE*

Abstract—We show that the coexistence of strong internal polarization and large carrier (i.e. electron and hole) effective mass accounts for ~51% of the efficiency droop under high current densities in traditional (hexagonal-phase) indium gallium aluminum nitride (InGaAlN) light-emitting diodes (h-LEDs) compared to cubic-phase InGaAlN LEDs (c-LEDs). Our analysis based on variational technique on c-LEDs predicts an enhancement of the current density at the onset of the droop, inherently present in green c-LEDs. These effects are a consequence of the polarization-free nature and small carrier effective mass of c-LEDs. Our analysis indicates that by overlooking the electron-hole wavefunction overlap, the well-known ABC-model is suspected to overestimate the Auger coefficient, leading to questionable conclusions on the efficiency droop. In turn, it shows that the c-LED efficiency droop is much immune to the Auger electron-hole asymmetry, the increase of Auger coefficient, and thus efficiency degradation mechanisms.

Index Terms— InGaAlN, light-emitting diode, cubic phase, efficiency droop, internal polarization

I. INTRODUCTION

NOWADAYS, white light-emitting diodes (LEDs) can reach ~200 lm/W, while still generating more heat than light. According to the traditional solid-state lighting (SSL) roadmap, these phosphor-converted LEDs have a theoretical luminous efficacy limit of 255 lm/W.[1] However, in these white LEDs, phosphors and secondary lenses degrade significantly their source efficiency, optical delivery efficiency, and spectral efficacy.[1], [2] A new and accelerated SSL roadmap to achieve an ultimate luminous efficacy of 414 lm/W can only succeed via color-mixing phosphor-free direct-emitting LEDs.[1] Amongst the visible LEDs, green LEDs are four

Manuscript received March 9, 2022. This work is supported by the National Science Foundation Faculty Early Career Development (CAREER) Program under award number NSF-ECCS-16-52871. The authors acknowledge the computational resources allocated by the Extreme Science and Engineering Discovery Environment (XSEDE) with No. TG-DMR180075. (Corresponding author: Can Bayram.)

Y.-C. Tsai, C. Bayram, and J.-P. Leburton are with the Department of Electrical and Computer Engineering, University of Illinois at Urbana-Champaign, Urbana, IL 61801 USA, and also with the Holonyak Micro and Nanotechnology Laboratory, University of Illinois at Urbana-Champaign, Urbana, IL 61801 USA (e-mail: yichiats2@illinois.edu; cbayram@illinois.edu).

J.-P. Leburton is also with the Department of Physics, University of Illinois at Urbana-Champaign, Urbana, IL 61801 USA (e-mail: jleburto@illinois.edu).

times less efficient than their blue counterparts, and suffer the most from an efficiency droop (i.e. an efficiency rollover as the current density increases once the maximum internal quantum efficiency (IQE) has been reached). Auger recombination, electron leakage, and internal polarization are among the mechanisms proposed to explain this efficiency degradation. Recent experiments on traditional (hexagonal-phase) indium gallium aluminum nitride (InGaAlN) LEDs (h-LEDs) reported hot-carrier emission from the InGaN quantum wells (QWs), implying strong Auger recombination, even under a low current density of ~1.6 A/cm².[3] The strong Auger recombination is typically attributed to a large Auger coefficient of 10⁻³⁰ cm⁶s⁻¹, enhanced by phonon scattering,[4] alloy scattering,[4] and interface roughness scattering.[5] However, this explanation is inconsistent with the low efficiency droop in gallium arsenide (GaAs)- and gallium phosphide (GaP)-based LEDs, that have similar Auger coefficients.[6]–[8] Moreover, in h-LEDs, the efficiency droop increases as the emission wavelength (and the indium mole fraction) increases from blue to green, which cannot be explained by the large Auger coefficient value alone.

In this paper, the inherent causes of the efficiency droop and low current density at the onset of the efficiency droop in green h-LEDs and cubic-phase (instead of traditional, hexagonal-phase) InGaAlN LEDs (c-LEDs) are investigated by computational modeling. We find that the coexistence of strong internal polarization and large carrier (i.e. electron and hole) effective mass induces strong Auger recombination that causes the large performance rollover in h-LEDs. On the opposite, in c-LEDs, the absence of internal polarization together with smaller carrier effective mass weakens Auger recombination, which quenches the droop by ~51%. These findings point at new ways to improve the performances of green LEDs.

II. COMPUTATIONAL DETAILS

For the sake of performance comparison, a h-LED and a c-LED are simulated with the following structure configuration: 120-nm-thick *n*-type GaN:Si [Si concentration of 10¹⁸ cm⁻³] / 10-nm-thick *i*-GaN barrier / 3-nm *i*-In_{0.30}Ga_{0.70}N single QW / 10-nm-thick *i*-GaN barrier / 15-nm *p*-Al_{0.2}Ga_{0.8}N:Mg [Mg concentration of 5×10¹⁹ cm⁻³] / 100-nm-thick *p*-GaN:Mg [Mg concentration of 10¹⁹ cm⁻³] / 15-nm-thick *p*⁺-GaN:Mg [Mg concentration of 10²⁰ cm⁻³]. A schematic of both LED structures is shown on top of Fig. 1. Simulations are carried out by the recently developed Open Boundary Quantum LED Simulator (OBQ-LEDsim),[9] for which a trial wavefunction is introduced to describe the ground state of finite barrier QWs in the LED active layers in the presence of electric fields:

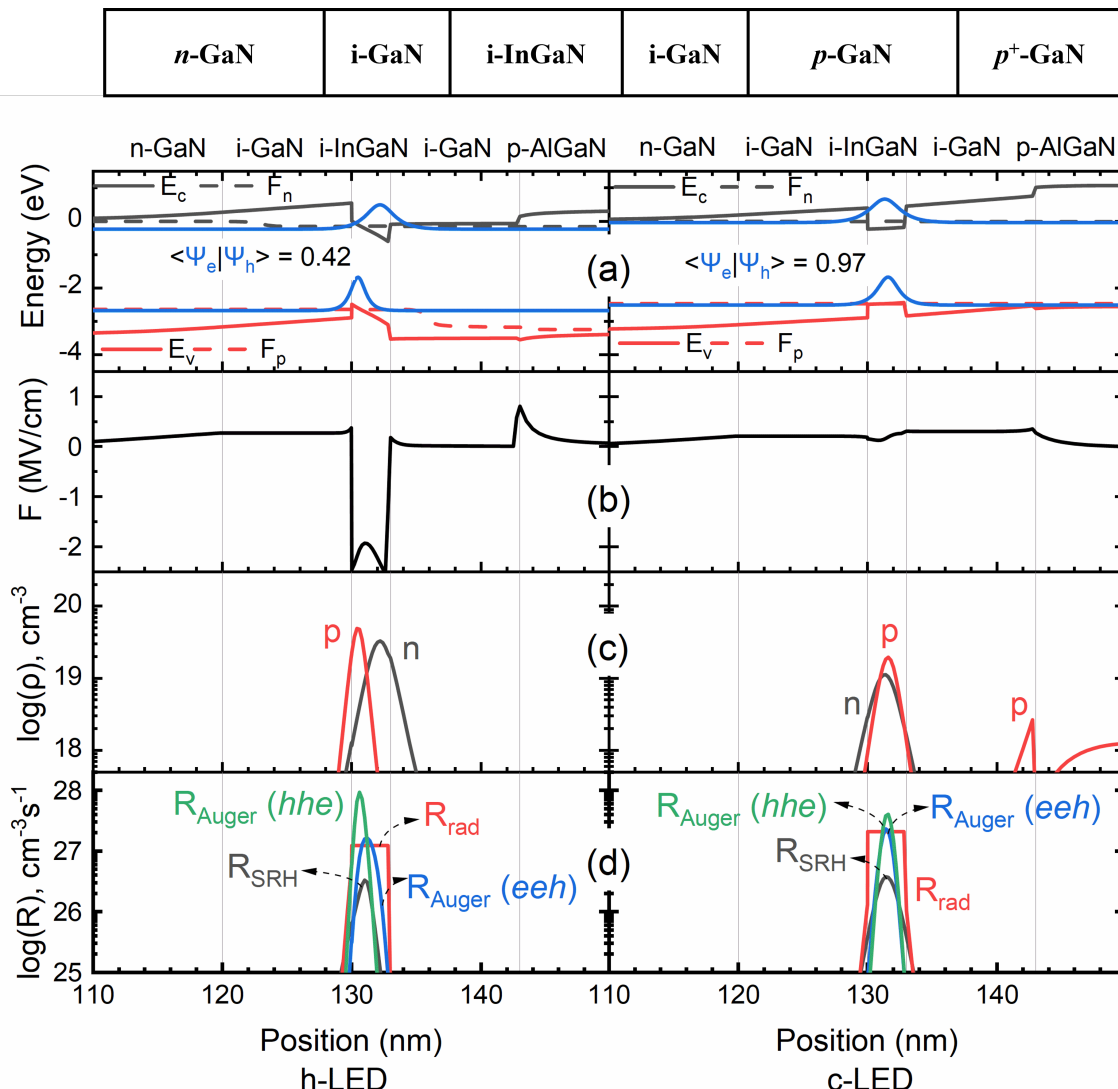


Fig. 1. The top schematic shows the device structure of the InGaAlN LEDs. (a) Band diagrams, (b) electric fields (F), (c) carrier concentrations (ρ), and (d) recombination rates (R) as a function of position under the current density of 200A/cm² for the hexagonal-phase (h-) InGaAlN LED and the cubic-phase (c-) InGaAlN LED are shown. The individual contributions of the recombination rates resulting from Shockley–Read–Hall (R_{SRH}), radiative (R_{rad}), eeh [$R_{Auger}(eeh)$] and hhe [$R_{Auger}(hhe)$] Auger recombination are also represented. The electron-hole wavefunction overlaps ($\langle \Psi_e | \Psi_h \rangle$) of h- and c-LEDs are 0.42 and 0.97, respectively. E_c, E_v, F_n, F_p, n, and p are conduction and valence band edges, quasi-Fermi levels for electron and hole, electron and hole densities, respectively.

$$\psi(x) = \sqrt{\frac{\beta^2}{2\pi\alpha}} \sin\left(\frac{\alpha\pi}{\beta}\right) \frac{e^{\alpha(x+\gamma)}}{\cosh[\beta(x+\gamma)]}, \quad (1)$$

where α , β , and γ are variational parameters associated with the wavefunction symmetry, width, and position, respectively. The condition $\alpha < \beta$ ensures the trial wavefunction vanishes at infinity, without the need of artificial boundaries. This variational approach is integrated with the classical drift-diffusion model within the OBQ-LEDsim by solving the Schrödinger–Poisson equations self-consistently, and by updating the overall electric potentials with the quantum potentials through the *Bohm* potential technique.[10] Our approach merges nicely quantum and continuum physical quantities without enforcing artificial boundaries between the QW and classical continuum, thereby enabling quantum carrier densities to be explicitly defined at arbitrary positions in LEDs.[11] The software details have been reported in our earlier work.[9], [11] Carrier degeneracy as well as phase-space

filling effects over the whole LED structures are considered by describing carrier densities using Fermi-Dirac statistics and by computing the spontaneous emission rates in the QW and in the classical continuum with Fermi’s golden rule, where the band-to-band optical transition matrix elements are derived from generalizing Kane’s model.[12], [13] The calculated radiative coefficients resulting from band-to-band recombination in h- and c-In_{0.3}Ga_{0.7}N under non-degenerate conditions are 1.73×10^{-11} cm³s⁻¹ and 3.14×10^{-11} cm³s⁻¹, respectively. The former value agrees with the measured values ranging from 1.4×10^{-11} cm³s⁻¹ to 2×10^{-11} cm³s⁻¹ that validates the accuracy of the model.[14] The latter value is twice larger than the former value, implying radiative efficiency in c-InGaN is higher than in h-InGaN, which was confirmed by prior measurements.[15] We attribute the superior radiative efficiency of c-InGaN to the reduced electron and hole effective masses compared to those in h-InGaN counterparts.[16] For nonradiative recombination, we assume a Shockley–Read–Hall

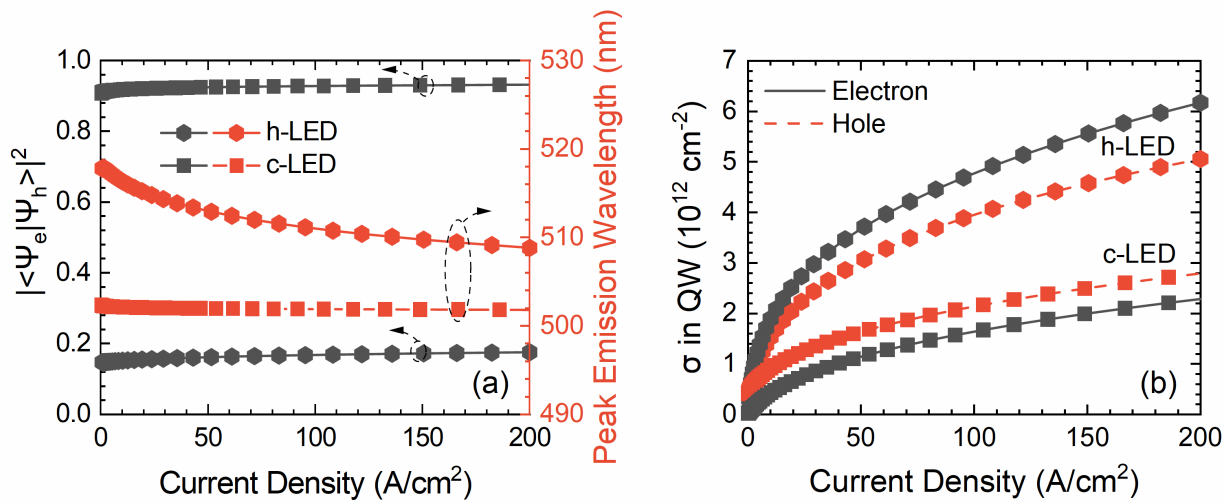


Fig. 2. (a) Squared electron-hole wavefunction overlap ($|\langle \psi_e | \psi_h \rangle|^2$) (left y-axis) and peak emission wavelength (right y-axis) and (b) electron and hole sheet charge densities (σ) in the quantum well (QW) as a function of current density for the hexagonal-phase (h-) and cubic-phase (c-) InGaN LEDs are shown.

(SRH) nonradiative lifetime (τ) of 18.5 ns, eeh (C_n) and hhe (C_p) Auger coefficients of 10^{-30} cm⁶s⁻¹, while ohmic contacts are assumed for both LEDs.[14], [17]–[19] It should be pointed out that the C_n and C_p in c-LEDs have not yet been reported in the literature. However, by comparing the electronic structure of c-GaN with that of h-GaN,[17], [21] one can see that c-GaN has significantly fewer energy states close to the conduction band minimum and the valence band maximum. In particular, the energy difference between the first and second conduction bands at the Γ point is >8 eV.[17], [20] These effects combined are expected to impede both direct and indirect Auger transitions, leading to lower C_n and C_p with respect to h-GaN. In our analysis of the individual contributions of internal polarization and carrier effective mass to the efficiency droop, we use the same C_n and C_p in both LEDs, thereby underestimating the c-LED performances.

III. RESULTS AND DISCUSSION

In Fig. 1, we show (a) spatially resolved band diagrams, (b) electric fields (F), (c) carrier densities (ρ), and (d) recombination rates (R) of the h- and c-LEDs operated under the same current density of 200 A/cm². As shown in Fig. 1(a) (left panel), the h-LED band edges tilt in the QW even with a high bias of 3.27V. Polarization-induced electric fields are the major reason that prevents the h-LED from achieving flat-band conditions. The electrons and holes in the h-LED are strongly localized within their respective QW, resulting in a small electron-hole wavefunction overlap of 0.42, which is half of its value in the c-LED (right panel). As seen in Fig. 1(b) (left panel), the spatially separated QW electrons and holes screen the polarization-induced electric fields, yielding a 1.93 MV/cm electric field in the QW center, whereas the extension of the overall electric field toward the QW edges reaches a maximum value of 2.43 MV/cm. The c-LED exhibits a different effect, where the electric field achieves its minimum value of 0.13 MV/cm on the left QW edge and gradually increases to its maximum value of 0.31 MV/cm on the right QW edge. This severe field dissimilarity between the h- and c-phases is due to poor electron-hole wavefunction overlap caused by the

presence of polarization field in the h-LED. Fig. 1(c) (left panel) shows the h-LED electrons and holes pile up in the QW, rising to peak densities of 3.30×10^{19} and 4.93×10^{19} cm⁻³, respectively. These values are more than twice of those in the c-LED (right panel). In the h-LED QW, the hole distribution is more localized than the electron distribution because the heavy hole mass (m_h^*) of 1.78 m₀ is ten times heavier than the electron effective mass (m_e^*) of 0.16 m₀ exhibiting a higher hole density peak than the electron density peak. It follows that the electron-hole wavefunction overlap in the QWs is influenced by the large m_h^* . Figure 1(d) displays the effects of poor electron-hole wavefunction overlap on SRH, radiative, eeh and hhe Auger recombination. It is seen that the strong hole localization caused by the coexistence of strong internal polarization and large hole effective mass in the h-LED (left panel) boosts the peak hole density and enhances the hhe Auger recombination. Interestingly, the hhe Auger recombination rates overcome the SRH, radiative, as well as the eeh Auger recombination rates, making it the dominant recombination channel because the hole distribution is more localized in the QW than the electron distribution. At the opposite, the electron-hole wavefunction overlap is enhanced in the c-LED (right panel) because of its polarization-free nature and its smaller hole effective mass, i.e. $m_h^* = 0.84$ m₀. In conclusion, increasing the electron-hole wavefunction overlap lowers peak carrier densities, weakens Auger recombination asymmetry, and enhances radiative recombination rate.

Figure 2(a) shows the squared electron-hole wavefunction overlap ($|\langle \psi_e | \psi_h \rangle|^2$) and the peak emission wavelength as a function of current density for both the h- and c-LEDs. Under a typical operational current density of 35 A/cm², the squared electron-hole wavefunction overlap in the h-LED is 17% of that in the c-LED. As the current density increases to 200 A/cm², the h-LED value increases to 19% of that in the c-LED. As mentioned above, the squared electron-hole wavefunction overlap is significantly lower in the h-LED than in the c-LED regardless of current densities because of the strong

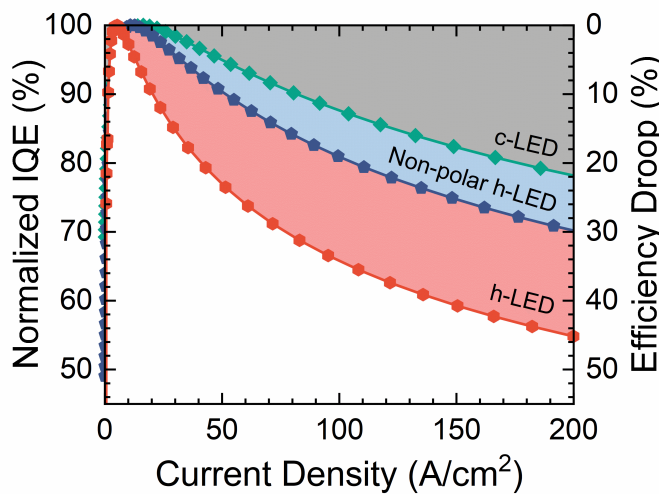


Fig. 3. Normalized internal quantum efficiency (IQE) (left y-axis) and efficiency droop (right y-axis) as a function of current density are plotted. Red hexagons and green rhombuses refer to the hexagonal-phase (h-) and cubic-phase (c-) InGaN LEDs, whereas blue pentagons refer to the non-polar h-LED grown on *m*-plane GaN substrates.

polarization-induced electric fields. The peak emission wavelength of h-LED blueshifts from 518 to 509 nm as the current density increases from 1 to 200 A/cm². In contrast, c-LED emits at ~502 nm with only a 0.2 nm blueshift for the same current density range. Figure 2(b) shows electron and hole sheet charge densities (σ) in the QW as a function of current density for the h- and c-LEDs. The electron and hole sheet charge densities of h-GaN are more than two times larger than those in the c-LED. This is again attributed to the large internal polarization of the h-LED. As described earlier, large internal polarization causes poor electron-hole wavefunction overlap, which requires higher QW carrier densities to achieve the same total recombination rate as in the absence of internal polarization.

In order to identify the individual contributions of internal polarization and carrier effective mass to the efficiency droop, we simulated one additional structure, i.e., a non-polar h-LED. The non-polar h-LED has the same h-LED device structure as described in Fig. 1 (left panel), but is grown on *m*-plane GaN substrates. Figure 3 displays the normalized IQE and efficiency droop of the three LEDs as a function of current density. The h-LED suffers from the poorest electron-hole wavefunction overlap, resulting in the highest efficiency droop of 45% under 200 A/cm². The efficiency droop is reduced to 29% (i.e. a 35% reduction) for the non-polar h-LED thanks to internal polarization elimination. It should be emphasized that the efficiency droop reduction in non-polar h-LEDs that was previously attributed to the decrease of carrier leakage from active region overlooks the interplay between internal polarization and Auger recombination.[22], [23] Indeed, recent experiments suggest that the efficiency droop reduction in non-polar h-LEDs is in fact due to carrier delocalization, (a situation different than in polar h-LEDs) that results in stronger electron-hole wavefunction overlap, lower QW carrier densities, and lower Auger recombination rates.[24] Switching from non-polar h-LEDs to c-LEDs further quenches the efficiency droop from 29% to 22% (i.e. a 24% reduction). This reduction is primarily due to the increased band-to-band optical transition matrix element and electron-hole wavefunction

overlap. We attributed the increase of the band-to-band optical transition matrix element (electron-hole wavefunction overlap) to the decrease in m_e^* (m_h^*) from 0.16 (1.78) m_0 in the h-LED to 0.13 (0.84) m_0 in the c-LED. Overall, the efficiency droop in c-LEDs has been substantially reduced by ~51% with respect to the traditional h-LEDs by means of internal polarization elimination and carrier effective mass reduction. Such significant improvement indicates that the coexistence of strong internal polarization and large carrier effective mass is the major cause of the efficiency droop that cannot be solely explained by large Auger coefficient.

One cannot emphasize more the role of internal polarization on the wavefunction overlap on the onset of Auger recombination and its effect on the IQE, which is missing in the well-known ABC-model,[25] for which $n = p$ is a common approximation without consideration for the electron-hole wavefunction overlap. Despite the fact that the effective ambipolar Auger coefficient (C_a) in QWs is calculated by multiplying the bulk C_a value by the squared electron-hole wavefunction overlap,[26] prior studies have shown that disregarding this electron-hole wavefunction overlap would result in an overestimation of the C_a value.[27] This overestimation is observed in the present study, where we consider the influence of Auger electron-hole asymmetry ($C_n/C_p \neq 1$) on the efficiency droop. In a previous work, we reported that the efficiency droop significantly depends on Auger electron-hole asymmetry.[11] Because the individual (C_n, C_p) coefficients are actually undetermined, we show in Figs. 4(a) and (b) the color plots of the efficiency droop as a function of C_n and C_p , separately, and expressed in units of 2×10^{-30} cm⁶s⁻¹, under the current density of 200 A/cm² for the h- and c-LEDs, respectively. C_a expressed in units of 2×10^{-30} cm⁶s⁻¹ is shown as the dotted lines on these color plots. The efficiency droops of 45% and 22% for the h- and c-LEDs indicated by the dashed lines are chosen as references. They are calculated assuming Auger electron-hole symmetry ($C_n/C_p = 1$) and $C_a = 2 \times 10^{-30}$ cm⁶s⁻¹. It is seen that multiple combinations of (C_n, C_p) result in the same efficiency droop. Hence, in the h-LED, this can be obtained by either decreasing or increasing C_n/C_p and C_a simultaneously. In the c-LED, it is seen that this behavior is not observed as the efficiency droop depends solely on C_a regardless of the C_n/C_p ratio. This behavior difference between the h-LED and the c-LED is credited to strong Auger recombination asymmetry in h-LEDs, as explained in Fig. 1. As a result, an optimum C_n/C_p ratio in the h-LED could reduce the efficiency droop from 51% to 35% if $C_a = 2 \times 10^{-30}$ cm⁶s⁻¹. It is also pointed out that the impact of C_n/C_p uncertainty on the efficiency droop increases with increased C_a . Therefore, it appears highly improbable that in h-LEDs the efficiency droop is attributed to a single C_a value, without considering the impact of the electron-hole wavefunction overlap on the recombination mechanism. Asides from this later point, one can then conclude that the h-LEDs tend to exhibit stronger efficiency droop than c-LEDs with C_a increase. For instance, the h- and c-LEDs have both vanishing efficiency droop for $C_n = C_p = 0$ cm⁶s⁻¹. Yet, for $C_n = C_p = 3 \times 10^{-30}$ cm⁶s⁻¹, the efficiency droop in h-LED can reach up to 59%, which is nearly twice the 38% observed in the c-LED. Additionally, the fact that usual IQE degradations associated with defects, phonons, alloy disorders, and interface

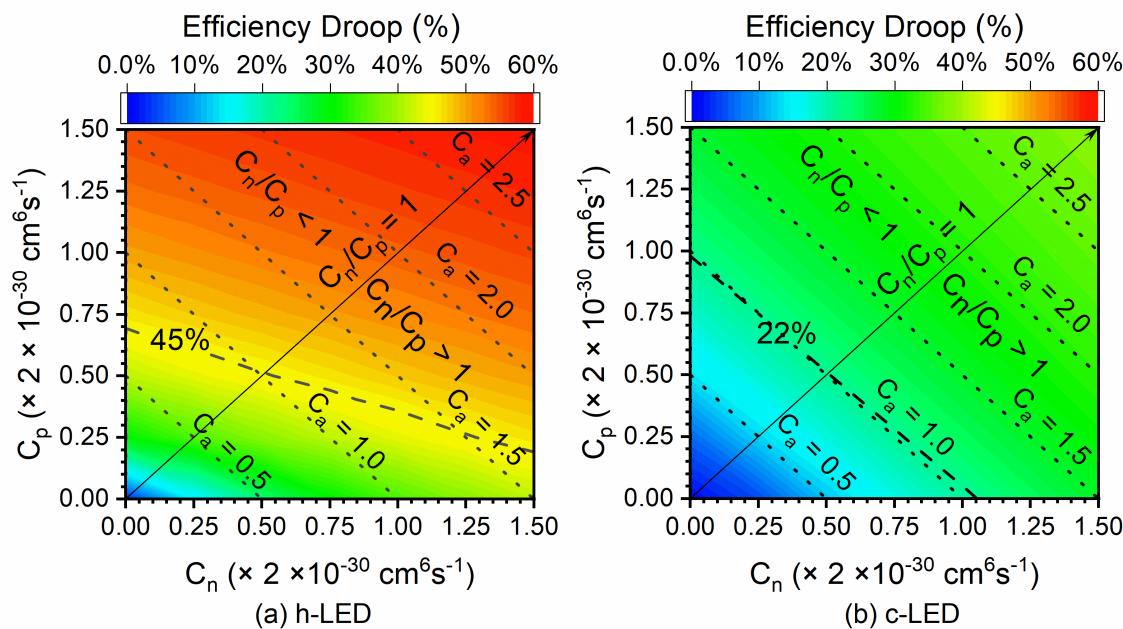


Fig. 4. Contour plots of the efficiency droop as a function of *eeh* (C_n) and *hhe* (C_p) Auger coefficients under the current density of $200\text{A}/\text{cm}^2$ for the (a) hexagonal-phase (h-) and (b) cubic-phase (c-) InGaAlN LEDs are shown. The ambipolar Auger coefficient (C_a) expressed in units of $2 \times 10^{-30} \text{ cm}^6 \text{s}^{-1}$ is shown as the dotted lines. The efficiency droops of 45% and 22% for the h- and c-LEDs are indicated by the dashed lines, respectively. They are calculated assuming Auger electron-hole symmetry ($C_n/C_p = 1$) and $C_a = 2 \times 10^{-30} \text{ cm}^6 \text{s}^{-1}$ and highlighted as references.

roughness,[4] are commonly linked to the increase of C_a , implies that the efficiency droop in h-LED is more sensitive to these degradation mechanisms than the c-LED. For these reasons, c-LEDs offer an appropriate solution to reduce the impact of these degradation effects on the efficiency droop, resulting in more efficient green LEDs than h-LEDs. Moreover, in h-LEDs, wavelengths longer than blue (i.e. >450 nm) are achieved by increasing the indium composition in the QW. This process, unfortunately, further enhances internal polarization, increases hole effective mass, and deteriorates electron-hole wavefunction overlap, which explains why green LEDs have stronger efficiency droop than blue ones.

IV. CONCLUSION

In conclusion, Open Boundary Quantum LED Simulator-based analysis confirms that a large electron-hole wavefunction overlap is critical for achieving optimal internal quantum efficiency in green LEDs. It is shown that, in c-LEDs, the absence of internal polarization combined with the existence of small carrier effective mass contributes to enhancing electron-hole wavefunction overlap and lowering carrier densities, thereby quenching the efficiency droop. These results indicate that the major cause of the efficiency degradation in green h-LEDs is the poor electron-hole wavefunction overlap and cannot be explained by the sole Auger coefficient value. In this context, the well-known ABC-model may inadvertently overestimate the Auger coefficient by overlooking the electron-hole wavefunction overlap, which leads to incorrect conclusions on the efficiency droop. In contrast, the c-LED efficiency droop is much immune to the indetermination of Auger electron-hole asymmetry, the increase of ambipolar Auger coefficient value, and is also more robust to the adverse effects of efficiency degradation mechanisms. Based on these considerations, one may surmise that absence of internal polarization and small carrier effective mass found in c-LEDs

would result in increasing current density at the onset of the efficiency droop and reduce the efficiency droop by $\sim 51\%$ (w.r.t. h-LEDs) under high current densities. Introducing more QWs in c-LEDs could further reduce QW carrier densities and quench the efficiency droop since carrier delocalization and homogeneous injection are enabled in multiple QWs by the lack of internal polarization and carrier effective mass reduction.

REFERENCES

- [1] M. Pattison, M. Hansen, N. Bardsley, C. Elliott, K. Lee, L. Pattison, and J. Tsao, "2019 Lighting R&D Opportunities," Jan. 2020. doi: 10.2172/1618035.
- [2] A. L. Hicks, T. L. Theis, and M. L. Zellner, "Emergent Effects of Residential Lighting Choices: Prospects for Energy Savings," *J. Ind. Ecol.*, vol. 19, no. 2, pp. 285–295, Apr. 2015, doi: 10.1111/JIEC.12281.
- [3] J. Iveland, L. Martinelli, J. Peretti, J. S. Speck, and C. Weisbuch, "Direct Measurement of Auger Electrons Emitted from a Semiconductor Light-Emitting Diode under Electrical Injection: Identification of the Dominant Mechanism for Efficiency Droop," *Phys. Rev. Lett.*, vol. 110, no. 17, p. 177406, Apr. 2013, doi: 10.1103/PhysRevLett.110.177406.
- [4] E. Kioupakis, D. Steiauf, P. Rinke, K. T. Delaney, and C. G. Van de Walle, "First-principles calculations of indirect Auger recombination in nitride semiconductors," *Phys. Rev. B*, vol. 92, no. 3, p. 035207, Jul. 2015, doi: 10.1103/PhysRevB.92.035207.
- [5] C.-K. Tan, W. Sun, J. J. Wierer, and N. Tansu, "Effect of interface roughness on Auger recombination in semiconductor quantum wells," *AIP Adv.*, vol. 7, no. 3, p. 035212, Mar. 2017, doi: 10.1063/1.4978777.
- [6] J. Cho, E. F. Schubert, and J. K. Kim, "Efficiency droop in light-emitting diodes: Challenges and counter measures," *Laser Photonics Rev.*, vol. 7, no. 3, pp. 408–421, 2013, doi: 10.1002/lpor.201200025.
- [7] R. Windisch, B. Dutta, M. Kuijk, A. Knobloch, S. Meinlschmidt, S. Schöberl, P. Kiesel, G. Borghs, G. H. Döhler, and P. Heremans, "40% Efficient Thin-Film Surface-Textured Light-Emitting Diodes By Optimization of Natural Lithography," *IEEE Trans. Electron Devices*, vol. 47, no. 7, pp. 1492–1498, 2000, doi: 10.1109/16.848298.
- [8] Jin Wang, P. von Allmen, J.-P. Leburton, and K. J. Linden, "Auger

recombination in long-wavelength strained-layer quantum-well structures," *IEEE J. Quantum Electron.*, vol. 31, no. 5, pp. 864–875, May 1995, doi: 10.1109/3.375931.

Y.-C. Tsai, C. Bayram, and J.-P. Leburton, "An Open Boundary Quantum LED Simulator (OBQ-LEDsim)," 2021. <http://obqledsim.ece.illinois.edu/>.

C. de Falco, E. Gatti, A. L. Lacaia, and R. Sacco, "Quantum-corrected drift-diffusion models for transport in semiconductor devices," *J. Comput. Phys.*, vol. 204, no. 2, pp. 533–561, Apr. 2005, doi: 10.1016/j.jcp.2004.10.029.

Y.-C. Tsai, C. Bayram, and J.-P. Leburton, "Effect of Auger Electron–Hole Asymmetry on the Efficiency Droop in InGaN Quantum Well Light-Emitting Diodes," *IEEE J. Quantum Electron.*, vol. 58, no. 1, pp. 1–9, Feb. 2022, doi: 10.1109/JQE.2021.3137822.

S. L. Chuang, "Optical gain of strained wurtzite GaN quantum-well lasers," *IEEE J. Quantum Electron.*, vol. 32, no. 10, pp. 1791–1800, 1996, doi: 10.1109/3.538786.

S. L. Chuang, *Physics of Photonic Devices*, 2nd ed. Wiley, 2009.

Y. C. Shen, G. O. Mueller, S. Watanabe, N. F. Gardner, A. Munkholm, and M. R. Krames, "Auger recombination in InGaN measured by photoluminescence," *Appl. Phys. Lett.*, vol. 91, no. 14, p. 141101, Oct. 2007, doi: 10.1063/1.2785135.

R. Liu, R. Schaller, C. Q. Chen, and C. Bayram, "High Internal Quantum Efficiency Ultraviolet Emission from Phase-Transition Cubic GaN Integrated on Nanopatterned Si(100)," *ACS Photonics*, vol. 5, no. 3, pp. 955–963, Mar. 2018, doi: 10.1021/acspophotonics.7b01231.

T. Trupke, M. A. Green, P. Würfel, P. P. Altermatt, A. Wang, J. Zhao, and R. Corkish, "Temperature dependence of the radiative recombination coefficient of intrinsic crystalline silicon," *J. Appl. Phys.*, vol. 94, no. 8, pp. 4930–4937, 2003, doi: 10.1063/1.1610231.

Y.-C. Tsai and C. Bayram, "Structural and Electronic Properties of Hexagonal and Cubic Phase AlGaN Alloys Investigated Using First Principles Calculations," *Sci. Rep.*, vol. 9, no. 1, p. 6583, Dec. 2019, doi: 10.1038/s41598-019-43113-w.

Y.-C. Tsai and C. Bayram, "Band Alignments of Ternary Wurtzite and Zincblende III-Nitrides Investigated by Hybrid Density Functional Theory," *ACS Omega*, vol. 5, no. 8, pp. 3917–3923, Mar. 2020, doi: 10.1021/acsomega.9b03353.

Y.-C. Tsai and C. Bayram, "Mitigate self-compensation with high crystal symmetry: A first-principles study of formation and activation of impurities in GaN," *Comput. Mater. Sci.*, vol. 190, no. 1, p. 110283, Apr. 2021, doi: 10.1016/j.commatsci.2021.110283.

K. T. Delaney, P. Rinke, and C. G. Van de Walle, "Auger recombination rates in nitrides from first principles," *Appl. Phys. Lett.*, vol. 94, no. 19, p. 191109, May 2009, doi: 10.1063/1.3133359.

R. B. Araujo, J. S. De Almeida, and A. Ferreira Da Silva, "Electronic properties of III-nitride semiconductors: A first-principles investigation using the Tran-Blaha modified Becke-Johnson potential," *J. Appl. Phys.*, vol. 114, no. 18, p. 183702, Nov. 2013, doi: 10.1063/1.4829674.

J. Piprek and S. Li, "Electron leakage effects on GaN-based light-emitting diodes," *Opt. Quantum Electron.*, vol. 42, no. 2, pp. 89–95, Jan. 2010, doi: 10.1007/s11082-011-9437-z.

D. Saguatti, L. Bidinelli, G. Verzellesi, M. Meneghini, G. Meneghesso, E. Zanoni, R. Butendeich, and B. Hahn, "Investigation of Efficiency-Droop Mechanisms in Multi-Quantum-Well InGaN/GaN Blue Light-Emitting Diodes," *IEEE Trans. Electron Devices*, vol. 59, no. 5, pp. 1402–1409, May 2012, doi: 10.1109/TED.2012.2186579.

M. Shahmohammadi, W. Liu, G. Rossbach, L. Lahourcade, A. Dussaigne, C. Bougerol, R. Butté, N. Grandjean, B. Deveaud, and G. Jacopin, "Enhancement of Auger recombination induced by carrier localization in InGaN/GaN quantum wells," *Phys. Rev. B*, vol. 95, no. 12, pp. 1–10, 2017, doi: 10.1103/PhysRevB.95.125314.

H. Y. Ryu, H. S. Kim, and J. I. Shim, "Rate equation analysis of efficiency droop in InGaN light-emitting diodes," *Appl. Phys. Lett.*, vol. 95, no. 8, pp. 8–11, 2009, doi: 10.1063/1.3216578.

E. Kioupakis, Q. Yan, D. Steiauf, and C. G. Van de Walle, "Temperature and carrier-density dependence of Auger and radiative recombination in nitride optoelectronic devices," *New J. Phys.*, vol. 15, no. 12, p. 125006, Dec. 2013, doi: 10.1088/1367-2630/15/12/125006.

J. Piprek, F. Römer, and B. Witzigmann, "On the uncertainty of the Auger recombination coefficient extracted from InGaN/GaN light-emitting diode efficiency droop measurements," *Appl. Phys. Lett.*, vol. 106, no. 10, p. 101101, Mar. 2015, doi: 10.1063/1.4914833.

Quenching of the Efficiency Droop in Cubic Phase InGaAlN Light-Emitting Diodes

Yi-Chia Tsai, Jean-Pierre Leburton, *Life Fellow, IEEE*,
and Can Bayram, *Senior Member, IEEE*

Abstract—We show that the coexistence of strong internal polarization and large carrier (i.e. electron and hole) effective mass accounts for ~51% of the efficiency droop under high current densities in traditional (hexagonal-phase) indium gallium aluminum nitride (InGaAlN) light-emitting diodes (h-LEDs) compared to cubic-phase InGaAlN LEDs (c-LEDs). Our analysis based on variational technique on c-LEDs predicts an enhancement of the current density at the onset of the droop, inherently present in green c-LEDs. These effects are a consequence of the polarization-free nature and small carrier effective mass of c-LEDs. Our analysis indicates that by overlooking the electron-hole wavefunction overlap, the well-known ABC-model is suspected to overestimate the Auger coefficient, leading to questionable conclusions on the efficiency droop. In turn, it shows that the c-LED efficiency droop is much immune to the Auger electron-hole asymmetry, the increase of Auger coefficient, and thus efficiency degradation mechanisms.

Index Terms— InGaAlN, light-emitting diode, cubic phase, efficiency droop, internal polarization

I. INTRODUCTION

NOWADAYS, white light-emitting diodes (LEDs) can reach ~200 lm/W, while still generating more heat than light. According to the traditional solid-state lighting (SSL) roadmap, these phosphor-converted LEDs have a theoretical luminous efficacy limit of 255 lm/W.[1] However, in these white LEDs, phosphors and secondary lenses degrade significantly their source efficiency, optical delivery efficiency, and spectral efficacy.[1], [2] A new and accelerated SSL roadmap to achieve an ultimate luminous efficacy of 414 lm/W can only succeed via color-mixing phosphor-free direct-emitting LEDs.[1] Amongst the visible LEDs, green LEDs are four

Manuscript received March 9, 2022. This work is supported by the National Science Foundation Faculty Early Career Development (CAREER) Program under award number NSF-ECCS-16-52871. The authors acknowledge the computational resources allocated by the Extreme Science and Engineering Discovery Environment (XSEDE) with No. TG-DMR180075. (Corresponding author: Can Bayram.)

Y.-C. Tsai, C. Bayram, and J.-P. Leburton are with the Department of Electrical and Computer Engineering, University of Illinois at Urbana-Champaign, Urbana, IL 61801 USA, and also with the Holonyak Micro and Nanotechnology Laboratory, University of Illinois at Urbana-Champaign, Urbana, IL 61801 USA (e-mail: yichiats2@illinois.edu; cbayram@illinois.edu).

J.-P. Leburton is also with the Department of Physics, University of Illinois at Urbana-Champaign, Urbana, IL 61801 USA (e-mail: jleburto@illinois.edu).

times less efficient than their blue counterparts, and suffer the most from an efficiency droop (i.e. an efficiency rollover as the current density increases once the maximum internal quantum efficiency (IQE) has been reached). Auger recombination, electron leakage, and internal polarization are among the mechanisms proposed to explain this efficiency degradation. Recent experiments on traditional (hexagonal-phase) indium gallium aluminum nitride (InGaAlN) LEDs (h-LEDs) reported hot-carrier emission from the InGaN quantum wells (QWs), implying strong Auger recombination, even under a low current density of ~1.6 A/cm².[3] The strong Auger recombination is typically attributed to a large Auger coefficient of 10⁻³⁰ cm⁶s⁻¹, enhanced by phonon scattering,[4] alloy scattering,[4] and interface roughness scattering.[5] However, this explanation is inconsistent with the low efficiency droop in gallium arsenide (GaAs)- and gallium phosphide (GaP)-based LEDs, that have similar Auger coefficients.[6]–[8] Moreover, in h-LEDs, the efficiency droop increases as the emission wavelength (and the indium mole fraction) increases from blue to green, which cannot be explained by the large Auger coefficient value alone.

In this paper, the inherent causes of the efficiency droop and low current density at the onset of the efficiency droop in green h-LEDs and cubic-phase (instead of traditional, hexagonal-phase) InGaAlN LEDs (c-LEDs) are investigated by computational modeling. We find that the coexistence of strong internal polarization and large carrier (i.e. electron and hole) effective mass induces strong Auger recombination that causes the large performance rollover in h-LEDs. On the opposite, in c-LEDs, the absence of internal polarization together with smaller carrier effective mass weakens Auger recombination, which quenches the droop by ~51%. These findings point at new ways to improve the performances of green LEDs.

II. COMPUTATIONAL DETAILS

For the sake of performance comparison, a h-LED and a c-LED are simulated with the following structure configuration: 120-nm-thick *n*-type GaN:Si [Si concentration of 10¹⁸ cm⁻³] / 10-nm-thick *i*-GaN barrier / 3-nm *i*-In_{0.30}Ga_{0.70}N single QW / 10-nm-thick *i*-GaN barrier / 15-nm *p*-Al_{0.2}Ga_{0.8}N:Mg [Mg concentration of 5×10¹⁹ cm⁻³] / 100-nm-thick *p*-GaN:Mg [Mg concentration of 10¹⁹ cm⁻³] / 15-nm-thick *p*⁺-GaN:Mg [Mg concentration of 10²⁰ cm⁻³]. A schematic of both LED structures is shown on top of Fig. 1. Simulations are carried out by the recently developed Open Boundary Quantum LED Simulator (OBQ-LEDsim),[9] for which a trial wavefunction is introduced to describe the ground state of finite barrier QWs in the LED active layers in the presence of electric fields:

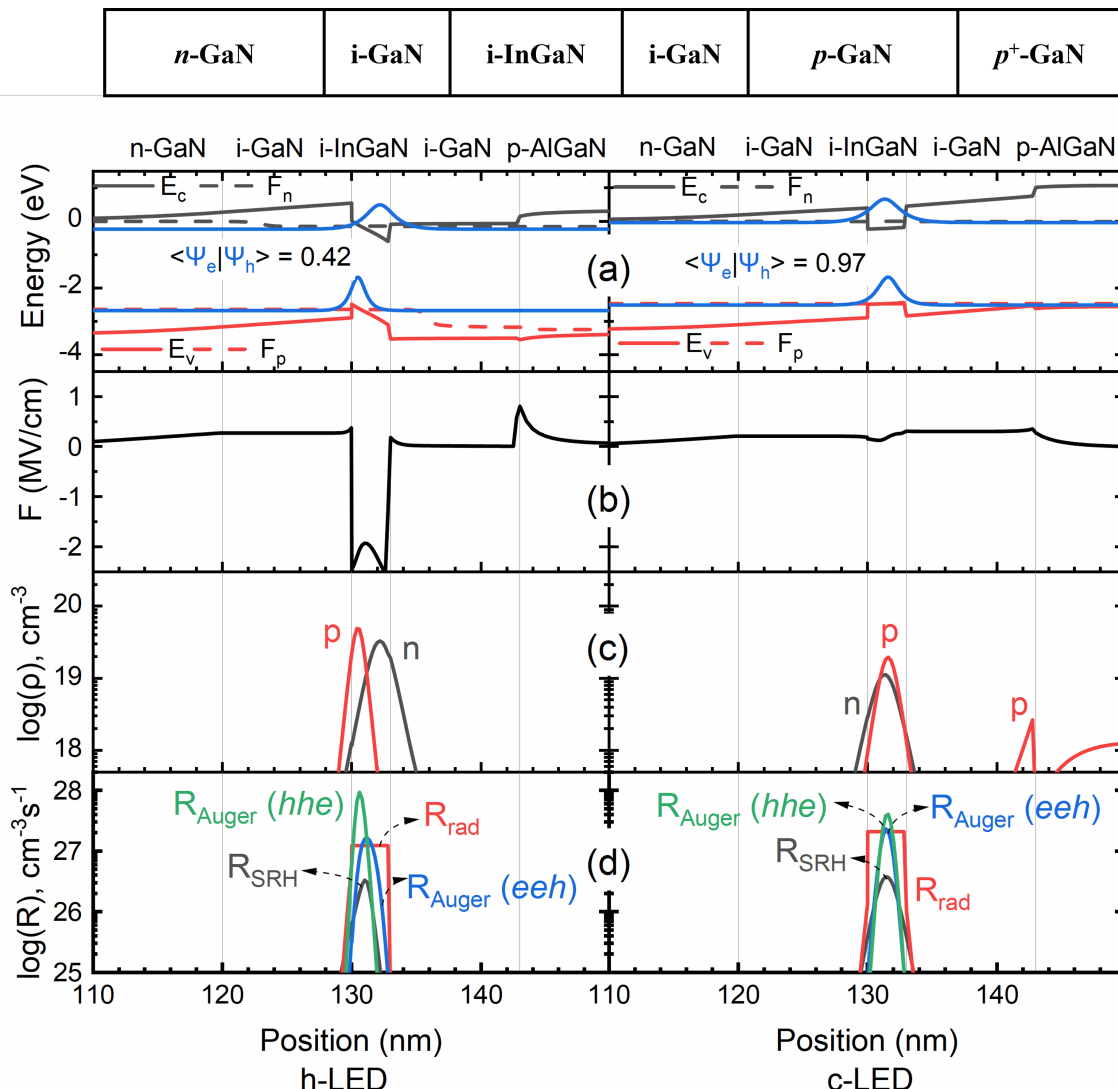


Fig. 1. The top schematic shows the device structure of the InGaAlN LEDs. (a) Band diagrams, (b) electric fields (F), (c) carrier concentrations (ρ), and (d) recombination rates (R) as a function of position under the current density of $200\text{A}/\text{cm}^2$ for the hexagonal-phase (h-) InGaAlN LED and the cubic-phase (c-) InGaAlN LED are shown. The individual contributions of the recombination rates resulting from Shockley–Read–Hall (R_{SRH}), radiative (R_{rad}), eeh [$R_{\text{Auger}}(\text{eeh})$] and hhe [$R_{\text{Auger}}(\text{hhe})$] Auger recombination are also represented. The electron-hole wavefunction overlaps ($\langle \Psi_e | \Psi_h \rangle$) of h- and c-LEDs are 0.42 and 0.97, respectively. E_c, E_v, F_n, F_p, n, and p are conduction and valence band edges, quasi-Fermi levels for electron and hole, electron and hole densities, respectively.

$$\psi(x) = \sqrt{\frac{\beta^2}{2\pi\alpha}} \sin\left(\frac{\alpha\pi}{\beta}\right) \frac{e^{\alpha(x+\gamma)}}{\cosh[\beta(x+\gamma)]}, \quad (1)$$

where α , β , and γ are variational parameters associated with the wavefunction symmetry, width, and position, respectively. The condition $\alpha < \beta$ ensures the trial wavefunction vanishes at infinity, without the need of artificial boundaries. This variational approach is integrated with the classical drift-diffusion model within the OBQ-LEDsim by solving the Schrödinger–Poisson equations self-consistently, and by updating the overall electric potentials with the quantum potentials through the *Bohm* potential technique.[10] Our approach merges nicely quantum and continuum physical quantities without enforcing artificial boundaries between the QW and classical continuum, thereby enabling quantum carrier densities to be explicitly defined at arbitrary positions in LEDs.[11] The software details have been reported in our earlier work.[9], [11] Carrier degeneracy as well as phase-space

filling effects over the whole LED structures are considered by describing carrier densities using Fermi-Dirac statistics and by computing the spontaneous emission rates in the QW and in the classical continuum with Fermi’s golden rule, where the band-to-band optical transition matrix elements are derived from generalizing Kane’s model.[12], [13] The calculated radiative coefficients resulting from band-to-band recombination in h- and c-In_{0.3}Ga_{0.7}N under non-degenerate conditions are $1.73 \times 10^{-11} \text{ cm}^3\text{s}^{-1}$ and $3.14 \times 10^{-11} \text{ cm}^3\text{s}^{-1}$, respectively. The former value agrees with the measured values ranging from $1.4 \times 10^{-11} \text{ cm}^3\text{s}^{-1}$ to $2 \times 10^{-11} \text{ cm}^3\text{s}^{-1}$ that validates the accuracy of the model.[14] The latter value is twice larger than the former value, implying radiative efficiency in c-InGaN is higher than in h-InGaN, which was confirmed by prior measurements.[15] We attribute the superior radiative efficiency of c-InGaN to the reduced electron and hole effective masses compared to those in h-InGaN counterparts.[16] For nonradiative recombination, we assume a Shockley–Read–Hall

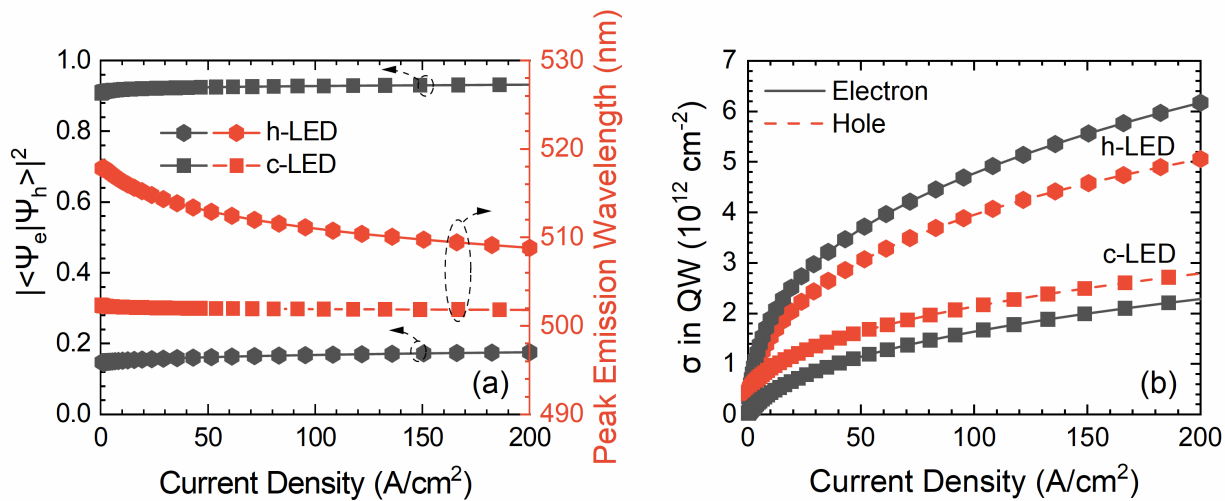


Fig. 2. (a) Squared electron-hole wavefunction overlap ($|\langle \psi_e | \psi_h \rangle|^2$) (left y-axis) and peak emission wavelength (right y-axis) and (b) electron and hole sheet charge densities (σ) in the quantum well (QW) as a function of current density for the hexagonal-phase (h-) and cubic-phase (c-) InGaN LEDs are shown.

(SRH) nonradiative lifetime (τ) of 18.5 ns, eeh (C_n) and hhe (C_p) Auger coefficients of $10^{-30} \text{ cm}^6 \text{s}^{-1}$, while ohmic contacts are assumed for both LEDs.[14], [17]–[19] It should be pointed out that the C_n and C_p in c-LEDs have not yet been reported in the literature. However, by comparing the electronic structure of c-GaN with that of h-GaN,[17], [21] one can see that c-GaN has significantly fewer energy states close to the conduction band minimum and the valence band maximum. In particular, the energy difference between the first and second conduction bands at the Γ point is >8 eV.[17], [20] These effects combined are expected to impede both direct and indirect Auger transitions, leading to lower C_n and C_p with respect to h-GaN. In our analysis of the individual contributions of internal polarization and carrier effective mass to the efficiency droop, we use the same C_n and C_p in both LEDs, thereby underestimating the c-LED performances.

III. RESULTS AND DISCUSSION

In Fig. 1, we show (a) spatially resolved band diagrams, (b) electric fields (F), (c) carrier densities (ρ), and (d) recombination rates (R) of the h- and c-LEDs operated under the same current density of 200 A/cm². As shown in Fig. 1(a) (left panel), the h-LED band edges tilt in the QW even with a high bias of 3.27V. Polarization-induced electric fields are the major reason that prevents the h-LED from achieving flat-band conditions. The electrons and holes in the h-LED are strongly localized within their respective QW, resulting in a small electron-hole wavefunction overlap of 0.42, which is half of its value in the c-LED (right panel). As seen in Fig. 1(b) (left panel), the spatially separated QW electrons and holes screen the polarization-induced electric fields, yielding a 1.93 MV/cm electric field in the QW center, whereas the extension of the overall electric field toward the QW edges reaches a maximum value of 2.43 MV/cm. The c-LED exhibits a different effect, where the electric field achieves its minimum value of 0.13 MV/cm on the left QW edge and gradually increases to its maximum value of 0.31 MV/cm on the right QW edge. This severe field dissimilarity between the h- and c-phases is due to poor electron-hole wavefunction overlap caused by the

presence of polarization field in the h-LED. Fig. 1(c) (left panel) shows the h-LED electrons and holes pile up in the QW, rising to peak densities of 3.30×10^{19} and $4.93 \times 10^{19} \text{ cm}^{-3}$, respectively. These values are more than twice of those in the c-LED (right panel). In the h-LED QW, the hole distribution is more localized than the electron distribution because the heavy hole mass (m_h^*) of 1.78 m_0 is ten times heavier than the electron effective mass (m_e^*) of 0.16 m_0 exhibiting a higher hole density peak than the electron density peak. It follows that the electron-hole wavefunction overlap in the QWs is influenced by the large m_h^* . Figure 1(d) displays the effects of poor electron-hole wavefunction overlap on SRH, radiative, eeh and hhe Auger recombination. It is seen that the strong hole localization caused by the coexistence of strong internal polarization and large hole effective mass in the h-LED (left panel) boosts the peak hole density and enhances the hhe Auger recombination. Interestingly, the hhe Auger recombination rates overcome the SRH, radiative, as well as the eeh Auger recombination rates, making it the dominant recombination channel because the hole distribution is more localized in the QW than the electron distribution. At the opposite, the electron-hole wavefunction overlap is enhanced in the c-LED (right panel) because of its polarization-free nature and its smaller hole effective mass, i.e. $m_h^* = 0.84 m_0$. In conclusion, increasing the electron-hole wavefunction overlap lowers peak carrier densities, weakens Auger recombination asymmetry, and enhances radiative recombination rate.

Figure 2(a) shows the squared electron-hole wavefunction overlap ($|\langle \psi_e | \psi_h \rangle|^2$) and the peak emission wavelength as a function of current density for both the h- and c-LEDs. Under a typical operational current density of 35 A/cm², the squared electron-hole wavefunction overlap in the h-LED is 17% of that in the c-LED. As the current density increases to 200 A/cm², the h-LED value increases to 19% of that in the c-LED. As mentioned above, the squared electron-hole wavefunction overlap is significantly lower in the h-LED than in the c-LED regardless of current densities because of the strong

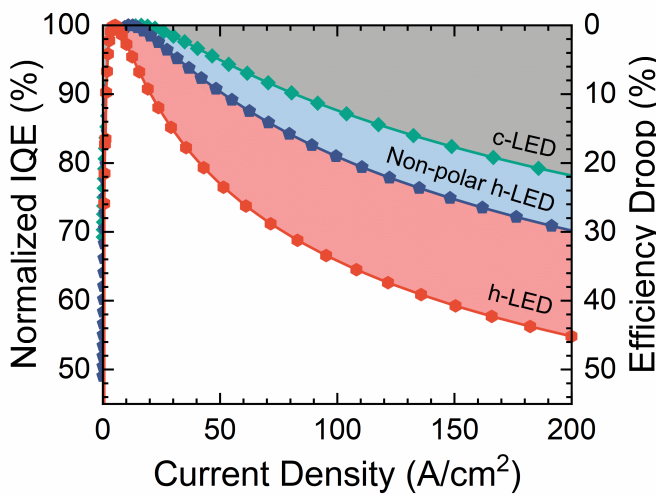


Fig. 3. Normalized internal quantum efficiency (IQE) (left y-axis) and efficiency droop (right y-axis) as a function of current density are plotted. Red hexagons and green rhombuses refer to the hexagonal-phase (h-) and cubic-phase (c-) InGaAlN LEDs, whereas blue pentagons refer to the non-polar h-LED grown on *m*-plane GaN substrates.

polarization-induced electric fields. The peak emission wavelength of h-LED blueshifts from 518 to 509 nm as the current density increases from 1 to 200 A/cm². In contrast, c-LED emits at ~502 nm with only a 0.2 nm blueshift for the same current density range. Figure 2(b) shows electron and hole sheet charge densities (σ) in the QW as a function of current density for the h- and c-LEDs. The electron and hole sheet charge densities of h-GaN are more than two times larger than those in the c-LED. This is again attributed to the large internal polarization of the h-LED. As described earlier, large internal polarization causes poor electron-hole wavefunction overlap, which requires higher QW carrier densities to achieve the same total recombination rate as in the absence of internal polarization.

In order to identify the individual contributions of internal polarization and carrier effective mass to the efficiency droop, we simulated one additional structure, i.e., a non-polar h-LED. The non-polar h-LED has the same h-LED device structure as described in Fig. 1 (left panel), but is grown on *m*-plane GaN substrates. Figure 3 displays the normalized IQE and efficiency droop of the three LEDs as a function of current density. The h-LED suffers from the poorest electron-hole wavefunction overlap, resulting in the highest efficiency droop of 45% under 200 A/cm². The efficiency droop is reduced to 29% (i.e. a 35% reduction) for the non-polar h-LED thanks to internal polarization elimination. It should be emphasized that the efficiency droop reduction in non-polar h-LEDs that was previously attributed to the decrease of carrier leakage from active region overlooks the interplay between internal polarization and Auger recombination.[22], [23] Indeed, recent experiments suggest that the efficiency droop reduction in non-polar h-LEDs is in fact due to carrier delocalization, (a situation different than in polar h-LEDs) that results in stronger electron-hole wavefunction overlap, lower QW carrier densities, and lower Auger recombination rates.[24] Switching from non-polar h-LEDs to c-LEDs further quenches the efficiency droop from 29% to 22% (i.e. a 24% reduction). This reduction is primarily due to the increased band-to-band optical transition matrix element and electron-hole wavefunction

overlap. We attributed the increase of the band-to-band optical transition matrix element (electron-hole wavefunction overlap) to the decrease in m_e^* (m_h^*) from 0.16 (1.78) m_0 in the h-LED to 0.13 (0.84) m_0 in the c-LED. Overall, the efficiency droop in c-LEDs has been substantially reduced by ~51% with respect to the traditional h-LEDs by means of internal polarization elimination and carrier effective mass reduction. Such significant improvement indicates that the coexistence of strong internal polarization and large carrier effective mass is the major cause of the efficiency droop that cannot be solely explained by large Auger coefficient.

One cannot emphasize more the role of internal polarization on the wavefunction overlap on the onset of Auger recombination and its effect on the IQE, which is missing in the well-known ABC-model,[25] for which $n = p$ is a common approximation without consideration for the electron-hole wavefunction overlap. Despite the fact that the effective ambipolar Auger coefficient (C_a) in QWs is calculated by multiplying the bulk C_a value by the squared electron-hole wavefunction overlap,[26] prior studies have shown that disregarding this electron-hole wavefunction overlap would result in an overestimation of the C_a value.[27] This overestimation is observed in the present study, where we consider the influence of Auger electron-hole asymmetry ($C_n/C_p \neq 1$) on the efficiency droop. In a previous work, we reported that the efficiency droop significantly depends on Auger electron-hole asymmetry.[11] Because the individual (C_n, C_p) coefficients are actually undetermined, we show in Figs. 4(a) and (b) the color plots of the efficiency droop as a function of C_n and C_p , separately, and expressed in units of 2×10^{-30} cm⁶s⁻¹, under the current density of 200 A/cm² for the h- and c-LEDs, respectively. C_a expressed in units of 2×10^{-30} cm⁶s⁻¹ is shown as the dotted lines on these color plots. The efficiency droops of 45% and 22% for the h- and c-LEDs indicated by the dashed lines are chosen as references. They are calculated assuming Auger electron-hole symmetry ($C_n/C_p = 1$) and $C_a = 2 \times 10^{-30}$ cm⁶s⁻¹. It is seen that multiple combinations of (C_n, C_p) result in the same efficiency droop. Hence, in the h-LED, this can be obtained by either decreasing or increasing C_n/C_p and C_a simultaneously. In the c-LED, it is seen that this behavior is not observed as the efficiency droop depends solely on C_a regardless of the C_n/C_p ratio. This behavior difference between the h-LED and the c-LED is credited to strong Auger recombination asymmetry in h-LEDs, as explained in Fig. 1. As a result, an optimum C_n/C_p ratio in the h-LED could reduce the efficiency droop from 51% to 35% if $C_a = 2 \times 10^{-30}$ cm⁶s⁻¹. It is also pointed out that the impact of C_n/C_p uncertainty on the efficiency droop increases with increased C_a . Therefore, it appears highly improbable that in h-LEDs the efficiency droop is attributed to a single C_a value, without considering the impact of the electron-hole wavefunction overlap on the recombination mechanism. Asides from this later point, one can then conclude that the h-LEDs tend to exhibit stronger efficiency droop than c-LEDs with C_a increase. For instance, the h- and c-LEDs have both vanishing efficiency droop for $C_n = C_p = 0$ cm⁶s⁻¹. Yet, for $C_n = C_p = 3 \times 10^{-30}$ cm⁶s⁻¹, the efficiency droop in h-LED can reach up to 59%, which is nearly twice the 38% observed in the c-LED. Additionally, the fact that usual IQE degradations associated with defects, phonons, alloy disorders, and interface

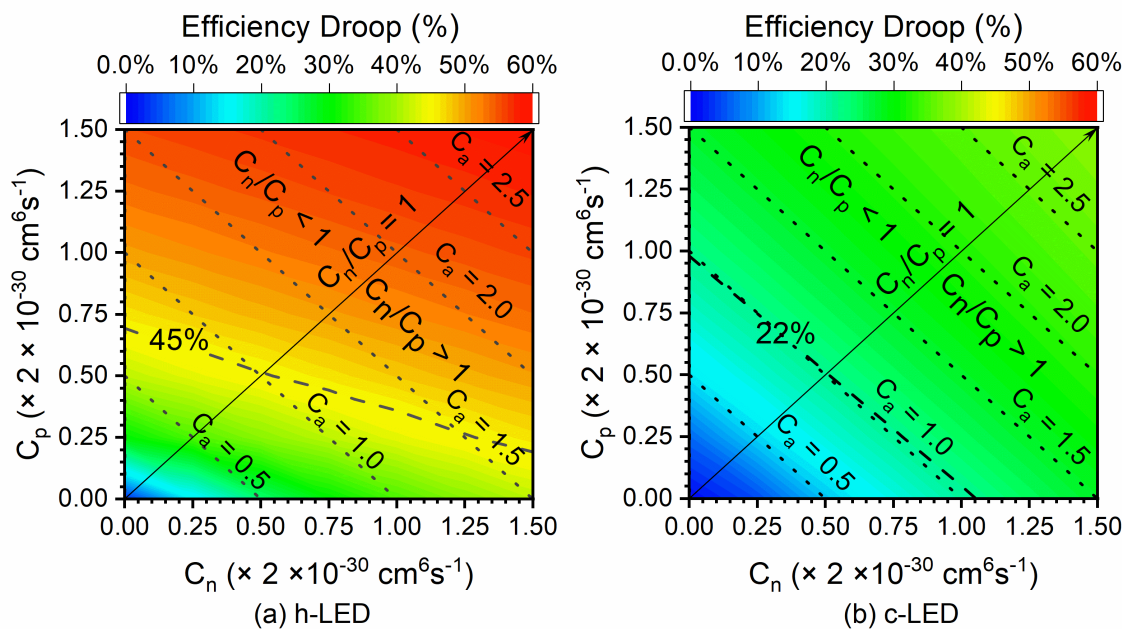


Fig. 4. Contour plots of the efficiency droop as a function of *eeh* (C_n) and *hhe* (C_p) Auger coefficients under the current density of $200\text{A}/\text{cm}^2$ for the (a) hexagonal-phase (h-) and (b) cubic-phase (c-) InGaAlN LEDs are shown. The ambipolar Auger coefficient (C_a) expressed in units of $2 \times 10^{-30} \text{ cm}^6 \text{s}^{-1}$ is shown as the dotted lines. The efficiency droops of 45% and 22% for the h- and c-LEDs are indicated by the dashed lines, respectively. They are calculated assuming Auger electron-hole symmetry ($C_n/C_p = 1$) and $C_a = 2 \times 10^{-30} \text{ cm}^6 \text{s}^{-1}$ and highlighted as references.

roughness,[4] are commonly linked to the increase of C_a , implies that the efficiency droop in h-LED is more sensitive to these degradation mechanisms than the c-LED. For these reasons, c-LEDs offer an appropriate solution to reduce the impact of these degradation effects on the efficiency droop, resulting in more efficient green LEDs than h-LEDs. Moreover, in h-LEDs, wavelengths longer than blue (i.e. >450 nm) are achieved by increasing the indium composition in the QW. This process, unfortunately, further enhances internal polarization, increases hole effective mass, and deteriorates electron-hole wavefunction overlap, which explains why green LEDs have stronger efficiency droop than blue ones.

IV. CONCLUSION

In conclusion, Open Boundary Quantum LED Simulator-based analysis confirms that a large electron-hole wavefunction overlap is critical for achieving optimal internal quantum efficiency in green LEDs. It is shown that, in c-LEDs, the absence of internal polarization combined with the existence of small carrier effective mass contributes to enhancing electron-hole wavefunction overlap and lowering carrier densities, thereby quenching the efficiency droop. These results indicate that the major cause of the efficiency degradation in green h-LEDs is the poor electron-hole wavefunction overlap and cannot be explained by the sole Auger coefficient value. In this context, the well-known ABC-model may inadvertently overestimate the Auger coefficient by overlooking the electron-hole wavefunction overlap, which leads to incorrect conclusions on the efficiency droop. In contrast, the c-LED efficiency droop is much immune to the indetermination of Auger electron-hole asymmetry, the increase of ambipolar Auger coefficient value, and is also more robust to the adverse effects of efficiency degradation mechanisms. Based on these considerations, one may surmise that absence of internal polarization and small carrier effective mass found in c-LEDs

would result in increasing current density at the onset of the efficiency droop and reduce the efficiency droop by $\sim 51\%$ (w.r.t. h-LEDs) under high current densities. Introducing more QWs in c-LEDs could further reduce QW carrier densities and quench the efficiency droop since carrier delocalization and homogeneous injection are enabled in multiple QWs by the lack of internal polarization and carrier effective mass reduction.

REFERENCES

- [1] M. Pattison, M. Hansen, N. Bardsley, C. Elliott, K. Lee, L. Pattison, and J. Tsao, "2019 Lighting R&D Opportunities," Jan. 2020. doi: 10.2172/1618035.
- [2] A. L. Hicks, T. L. Theis, and M. L. Zellner, "Emergent Effects of Residential Lighting Choices: Prospects for Energy Savings," *J. Ind. Ecol.*, vol. 19, no. 2, pp. 285–295, Apr. 2015, doi: 10.1111/JIEC.12281.
- [3] J. Iveland, L. Martinelli, J. Peretti, J. S. Speck, and C. Weisbuch, "Direct Measurement of Auger Electrons Emitted from a Semiconductor Light-Emitting Diode under Electrical Injection: Identification of the Dominant Mechanism for Efficiency Droop," *Phys. Rev. Lett.*, vol. 110, no. 17, p. 177406, Apr. 2013, doi: 10.1103/PhysRevLett.110.177406.
- [4] E. Kioupakis, D. Steiauf, P. Rinke, K. T. Delaney, and C. G. Van de Walle, "First-principles calculations of indirect Auger recombination in nitride semiconductors," *Phys. Rev. B*, vol. 92, no. 3, p. 035207, Jul. 2015, doi: 10.1103/PhysRevB.92.035207.
- [5] C.-K. Tan, W. Sun, J. J. Wierer, and N. Tansu, "Effect of interface roughness on Auger recombination in semiconductor quantum wells," *AIP Adv.*, vol. 7, no. 3, p. 035212, Mar. 2017, doi: 10.1063/1.4978777.
- [6] J. Cho, E. F. Schubert, and J. K. Kim, "Efficiency droop in light-emitting diodes: Challenges and counter measures," *Laser Photonics Rev.*, vol. 7, no. 3, pp. 408–421, 2013, doi: 10.1002/lpor.201200025.
- [7] R. Windisch, B. Dutta, M. Kuijk, A. Knobloch, S. Meinlschmidt, S. Schöberl, P. Kiesel, G. Borghs, G. H. Döhler, and P. Heremans, "40% Efficient Thin-Film Surface-Textured Light-Emitting Diodes By Optimization of Natural Lithography," *IEEE Trans. Electron Devices*, vol. 47, no. 7, pp. 1492–1498, 2000, doi: 10.1109/16.848298.
- [8] Jin Wang, P. von Allmen, J.-P. Leburton, and K. J. Linden, "Auger

1 recombination in long-wavelength strained-layer quantum-well
 2 structures," *IEEE J. Quantum Electron.*, vol. 31, no. 5, pp. 864–875,
 3 May 1995, doi: 10.1109/3.375931.

4 [9] Y.-C. Tsai, C. Bayram, and J.-P. Leburton, "An Open Boundary
 5 Quantum LED Simulator (OBQ-LEDsim)," 2021.
 6 <http://obqledsim.ece.illinois.edu/>.

7 [10] C. de Falco, E. Gatti, A. L. Lacaita, and R. Sacco,
 8 "Quantum-corrected drift-diffusion models for transport in
 9 semiconductor devices," *J. Comput. Phys.*, vol. 204, no. 2, pp.
 10 533–561, Apr. 2005, doi: 10.1016/j.jcp.2004.10.029.

11 [11] Y.-C. Tsai, C. Bayram, and J.-P. Leburton, "Effect of Auger
 12 Electron–Hole Asymmetry on the Efficiency Droop in InGaN
 13 Quantum Well Light-Emitting Diodes," *IEEE J. Quantum Electron.*,
 14 vol. 58, no. 1, pp. 1–9, Feb. 2022, doi: 10.1109/JQE.2021.3137822.

15 [12] S. L. Chuang, "Optical gain of strained wurtzite GaN quantum-well
 16 lasers," *IEEE J. Quantum Electron.*, vol. 32, no. 10, pp. 1791–1800,
 17 1996, doi: 10.1109/3.538786.

18 [13] S. L. Chuang, *Physics of Photonic Devices*, 2nd ed. Wiley, 2009.

19 [14] Y. C. Shen, G. O. Mueller, S. Watanabe, N. F. Gardner, A.
 20 Munkholm, and M. R. Krames, "Auger recombination in InGaN
 21 measured by photoluminescence," *Appl. Phys. Lett.*, vol. 91, no. 14,
 22 p. 141101, Oct. 2007, doi: 10.1063/1.2785135.

23 [15] R. Liu, R. Schaller, C. Q. Chen, and C. Bayram, "High Internal
 24 Quantum Efficiency Ultraviolet Emission from Phase-Transition
 25 Cubic GaN Integrated on Nanopatterned Si(100)," *ACS Photonics*,
 26 vol. 5, no. 3, pp. 955–963, Mar. 2018, doi:
 27 10.1021/acspophotonics.7b01231.

28 [16] T. Trupke, M. A. Green, P. Würfel, P. P. Altermatt, A. Wang, J.
 29 Zhao, and R. Corkish, "Temperature dependence of the radiative
 30 recombination coefficient of intrinsic crystalline silicon," *J. Appl.
 31 Phys.*, vol. 94, no. 8, pp. 4930–4937, 2003, doi: 10.1063/1.1610231.

32 [17] Y.-C. Tsai and C. Bayram, "Structural and Electronic Properties of
 33 Hexagonal and Cubic Phase AlGaN Alloys Investigated Using
 34 First Principles Calculations," *Sci. Rep.*, vol. 9, no. 1, p. 6583, Dec.
 35 2019, doi: 10.1038/s41598-019-43113-w.

36 [18] Y.-C. Tsai and C. Bayram, "Band Alignments of Ternary Wurtzite
 37 and Zincblende III-Nitrides Investigated by Hybrid Density
 38 Functional Theory," *ACS Omega*, vol. 5, no. 8, pp. 3917–3923, Mar.
 39 2020, doi: 10.1021/acsomega.9b03353.

40 [19] Y.-C. Tsai and C. Bayram, "Mitigate self-compensation with high
 41 crystal symmetry: A first-principles study of formation and activation
 42 of impurities in GaN," *Comput. Mater. Sci.*, vol. 190, no. 1, p.
 43 110283, Apr. 2021, doi: 10.1016/j.commatsci.2021.110283.

44 [20] K. T. Delaney, P. Rinke, and C. G. Van de Walle, "Auger
 45 recombination rates in nitrides from first principles," *Appl. Phys.
 46 Lett.*, vol. 94, no. 19, p. 191109, May 2009, doi: 10.1063/1.3133359.

47 [21] R. B. Araujo, J. S. De Almeida, and A. Ferreira Da Silva, "Electronic
 48 properties of III-nitride semiconductors: A first-principles
 49 investigation using the Tran-Blaha modified Becke-Johnson
 50 potential," *J. Appl. Phys.*, vol. 114, no. 18, p. 183702, Nov. 2013, doi:
 51 10.1063/1.4829674.

52 [22] J. Piprek and S. Li, "Electron leakage effects on GaN-based
 53 light-emitting diodes," *Opt. Quantum Electron.*, vol. 42, no. 2, pp.
 54 89–95, Jan. 2010, doi: 10.1007/s11082-011-9437-z.

55 [23] D. Saguatti, L. Bidinelli, G. Verzellesi, M. Meneghini, G.
 56 Meneghesso, E. Zanoni, R. Butendeich, and B. Hahn, "Investigation
 57 of Efficiency-Droop Mechanisms in Multi-Quantum-Well
 58 InGaN/GaN Blue Light-Emitting Diodes," *IEEE Trans. Electron
 59 Devices*, vol. 59, no. 5, pp. 1402–1409, May 2012, doi:
 60 10.1109/TED.2012.2186579.

1 recombination in long-wavelength strained-layer quantum-well
 2 structures," *IEEE J. Quantum Electron.*, vol. 31, no. 5, pp. 864–875,
 3 May 1995, doi: 10.1109/3.375931.

4 [9] Y.-C. Tsai, C. Bayram, and J.-P. Leburton, "An Open Boundary
 5 Quantum LED Simulator (OBQ-LEDsim)," 2021.
 6 <http://obqledsim.ece.illinois.edu/>.

7 [10] C. de Falco, E. Gatti, A. L. Lacaita, and R. Sacco,
 8 "Quantum-corrected drift-diffusion models for transport in
 9 semiconductor devices," *J. Comput. Phys.*, vol. 204, no. 2, pp.
 10 533–561, Apr. 2005, doi: 10.1016/j.jcp.2004.10.029.

11 [11] Y.-C. Tsai, C. Bayram, and J.-P. Leburton, "Effect of Auger
 12 Electron–Hole Asymmetry on the Efficiency Droop in InGaN
 13 Quantum Well Light-Emitting Diodes," *IEEE J. Quantum Electron.*,
 14 vol. 58, no. 1, pp. 1–9, Feb. 2022, doi: 10.1109/JQE.2021.3137822.

15 [12] S. L. Chuang, "Optical gain of strained wurtzite GaN quantum-well
 16 lasers," *IEEE J. Quantum Electron.*, vol. 32, no. 10, pp. 1791–1800,
 17 1996, doi: 10.1109/3.538786.

18 [13] S. L. Chuang, *Physics of Photonic Devices*, 2nd ed. Wiley, 2009.

19 [14] Y. C. Shen, G. O. Mueller, S. Watanabe, N. F. Gardner, A.
 20 Munkholm, and M. R. Krames, "Auger recombination in InGaN
 21 measured by photoluminescence," *Appl. Phys. Lett.*, vol. 91, no. 14,
 22 p. 141101, Oct. 2007, doi: 10.1063/1.2785135.

23 [15] R. Liu, R. Schaller, C. Q. Chen, and C. Bayram, "High Internal
 24 Quantum Efficiency Ultraviolet Emission from Phase-Transition
 25 Cubic GaN Integrated on Nanopatterned Si(100)," *ACS Photonics*,
 26 vol. 5, no. 3, pp. 955–963, Mar. 2018, doi:
 27 10.1021/acspophotonics.7b01231.

28 [16] T. Trupke, M. A. Green, P. Würfel, P. P. Altermatt, A. Wang, J.
 29 Zhao, and R. Corkish, "Temperature dependence of the radiative
 30 recombination coefficient of intrinsic crystalline silicon," *J. Appl.
 31 Phys.*, vol. 94, no. 8, pp. 4930–4937, 2003, doi: 10.1063/1.1610231.

32 [17] Y.-C. Tsai and C. Bayram, "Structural and Electronic Properties of
 33 Hexagonal and Cubic Phase AlGaN Alloys Investigated Using
 34 First Principles Calculations," *Sci. Rep.*, vol. 9, no. 1, p. 6583, Dec.
 35 2019, doi: 10.1038/s41598-019-43113-w.

36 [18] Y.-C. Tsai and C. Bayram, "Band Alignments of Ternary Wurtzite
 37 and Zincblende III-Nitrides Investigated by Hybrid Density
 38 Functional Theory," *ACS Omega*, vol. 5, no. 8, pp. 3917–3923, Mar.
 39 2020, doi: 10.1021/acsomega.9b03353.

40 [19] Y.-C. Tsai and C. Bayram, "Mitigate self-compensation with high
 41 crystal symmetry: A first-principles study of formation and activation
 42 of impurities in GaN," *Comput. Mater. Sci.*, vol. 190, no. 1, p.
 43 110283, Apr. 2021, doi: 10.1016/j.commatsci.2021.110283.

44 [20] K. T. Delaney, P. Rinke, and C. G. Van de Walle, "Auger
 45 recombination rates in nitrides from first principles," *Appl. Phys.
 46 Lett.*, vol. 94, no. 19, p. 191109, May 2009, doi: 10.1063/1.3133359.

47 [21] R. B. Araujo, J. S. De Almeida, and A. Ferreira Da Silva, "Electronic
 48 properties of III-nitride semiconductors: A first-principles
 49 investigation using the Tran-Blaha modified Becke-Johnson
 50 potential," *J. Appl. Phys.*, vol. 114, no. 18, p. 183702, Nov. 2013, doi:
 51 10.1063/1.4829674.

52 [22] J. Piprek and S. Li, "Electron leakage effects on GaN-based
 53 light-emitting diodes," *Opt. Quantum Electron.*, vol. 42, no. 2, pp.
 54 89–95, Jan. 2010, doi: 10.1007/s11082-011-9437-z.

55 [23] D. Saguatti, L. Bidinelli, G. Verzellesi, M. Meneghini, G.
 56 Meneghesso, E. Zanoni, R. Butendeich, and B. Hahn, "Investigation
 57 of Efficiency-Droop Mechanisms in Multi-Quantum-Well
 58 InGaN/GaN Blue Light-Emitting Diodes," *IEEE Trans. Electron
 59 Devices*, vol. 59, no. 5, pp. 1402–1409, May 2012, doi:
 60 10.1109/TED.2012.2186579.

1 recombination in long-wavelength strained-layer quantum-well
 2 structures," *IEEE J. Quantum Electron.*, vol. 31, no. 5, pp. 864–875,
 3 May 1995, doi: 10.1109/3.375931.

4 [9] Y.-C. Tsai, C. Bayram, and J.-P. Leburton, "An Open Boundary
 5 Quantum LED Simulator (OBQ-LEDsim)," 2021.
 6 <http://obqledsim.ece.illinois.edu/>.

7 [10] C. de Falco, E. Gatti, A. L. Lacaita, and R. Sacco,
 8 "Quantum-corrected drift-diffusion models for transport in
 9 semiconductor devices," *J. Comput. Phys.*, vol. 204, no. 2, pp.
 10 533–561, Apr. 2005, doi: 10.1016/j.jcp.2004.10.029.

11 [11] Y.-C. Tsai, C. Bayram, and J.-P. Leburton, "Effect of Auger
 12 Electron–Hole Asymmetry on the Efficiency Droop in InGaN
 13 Quantum Well Light-Emitting Diodes," *IEEE J. Quantum Electron.*,
 14 vol. 58, no. 1, pp. 1–9, Feb. 2022, doi: 10.1109/JQE.2021.3137822.

15 [12] S. L. Chuang, "Optical gain of strained wurtzite GaN quantum-well
 16 lasers," *IEEE J. Quantum Electron.*, vol. 32, no. 10, pp. 1791–1800,
 17 1996, doi: 10.1109/3.538786.

18 [13] S. L. Chuang, *Physics of Photonic Devices*, 2nd ed. Wiley, 2009.

19 [14] Y. C. Shen, G. O. Mueller, S. Watanabe, N. F. Gardner, A.
 20 Munkholm, and M. R. Krames, "Auger recombination in InGaN
 21 measured by photoluminescence," *Appl. Phys. Lett.*, vol. 91, no. 14,
 22 p. 141101, Oct. 2007, doi: 10.1063/1.2785135.

23 [15] R. Liu, R. Schaller, C. Q. Chen, and C. Bayram, "High Internal
 24 Quantum Efficiency Ultraviolet Emission from Phase-Transition
 25 Cubic GaN Integrated on Nanopatterned Si(100)," *ACS Photonics*,
 26 vol. 5, no. 3, pp. 955–963, Mar. 2018, doi:
 27 10.1021/acspophotonics.7b01231.

28 [16] T. Trupke, M. A. Green, P. Würfel, P. P. Altermatt, A. Wang, J.
 29 Zhao, and R. Corkish, "Temperature dependence of the radiative
 30 recombination coefficient of intrinsic crystalline silicon," *J. Appl.
 31 Phys.*, vol. 94, no. 8, pp. 4930–4937, 2003, doi: 10.1063/1.1610231.

32 [17] Y.-C. Tsai and C. Bayram, "Structural and Electronic Properties of
 33 Hexagonal and Cubic Phase AlGaN Alloys Investigated Using
 34 First Principles Calculations," *Sci. Rep.*, vol. 9, no. 1, p. 6583, Dec.
 35 2019, doi: 10.1038/s41598-019-43113-w.

36 [18] Y.-C. Tsai and C. Bayram, "Band Alignments of Ternary Wurtzite
 37 and Zincblende III-Nitrides Investigated by Hybrid Density
 38 Functional Theory," *ACS Omega*, vol. 5, no. 8, pp. 3917–3923, Mar.
 39 2020, doi: 10.1021/acsomega.9b03353.

40 [19] Y.-C. Tsai and C. Bayram, "Mitigate self-compensation with high
 41 crystal symmetry: A first-principles study of formation and activation
 42 of impurities in GaN," *Comput. Mater. Sci.*, vol. 190, no. 1, p.
 43 110283, Apr. 2021, doi: 10.1016/j.commatsci.2021.110283.

44 [20] K. T. Delaney, P. Rinke, and C. G. Van de Walle, "Auger
 45 recombination rates in nitrides from first principles," *Appl. Phys.
 46 Lett.*, vol. 94, no. 19, p. 191109, May 2009, doi: 10.1063/1.3133359.

48 [24] M. Shahmohammadi, W. Liu, G. Rossbach, L. Lahourcade, A.
 49 Dussaigne, C. Bougerol, R. Butté, N. Grandjean, B. Deveaud, and G.
 50 Jacobin, "Enhancement of Auger recombination induced by carrier
 51 localization in InGaN/GaN quantum wells," *Phys. Rev. B*, vol. 95, no.
 52 12, pp. 1–10, 2017, doi: 10.1103/PhysRevB.95.125314.

53 [25] H. Y. Ryu, H. S. Kim, and J. I. Shim, "Rate equation analysis of
 54 efficiency droop in InGaN light-emitting diodes," *Appl. Phys. Lett.*,
 55 vol. 95, no. 8, pp. 8–11, 2009, doi: 10.1063/1.3216578.

56 [26] E. Kioupakis, Q. Yan, D. Steiauf, and C. G. Van de Walle,
 57 "Temperature and carrier-density dependence of Auger and radiative
 58 recombination in nitride optoelectronic devices," *New J. Phys.*, vol.
 59 15, no. 12, p. 125006, Dec. 2013, doi:
 60 10.1088/1367-2630/15/12/125006.

57 [27] J. Piprek, F. Römer, and B. Witzigmann, "On the uncertainty of the
 58 Auger recombination coefficient extracted from InGaN/GaN
 59

60

light-emitting diode efficiency droop measurements," *Appl. Phys.
 Lett.*, vol. 106, no. 10, p. 101101, Mar. 2015, doi:
 10.1063/1.4914833.

1
2
3
4
5

Response to Reviewer #1's Comments

6
7**General comments:**

9 The paper theoretically investigates the improvement by the cubic-phase InGaAlN light-emitting
10 diodes (LEDs) and explores the possible causes of the efficiency droop in the traditional
11 hexagonal-phase LEDs. While the paper is purely theoretical, based only on simulations, the
12 manuscript is very well written, addressing all the relevant issues and providing fresh inputs on
13 the importance of the electron-hole wavefunction overlap and effective masses.

14
15 **R1:** I would only like to suggest Authors to consider adding some comments on how the present
16 conclusion and insight would carry to more realistic multiple-quantum-well-based LEDs as
17 opposed to the single-quantum-well cases examined herein.

18
19 **A:** We appreciate the Referee's positive and encouraging comments on our manuscript. Indeed,
20 one could hope that by adding more quantum wells (QW) in the device active region, this would
21 decrease their individual carrier densities and quench the efficiency droop under the same current
22 density. However, in h-LEDs, due to the coexistence of strong internal polarization and large hole
23 effective mass, charge carriers are captured and recombine primarily in the QWs close to the p-
24 contact.[1] Therefore, adding more QWs does not significantly reduce the efficiency droop. In
25 contrast, the lack of internal polarization and carrier effective mass reduction exhibited in c-LEDs
26 enable homogeneous injection in multiple QWs. In this case, the efficiency droop can be reduced
27 by adding more QWs. We have simulated and confirmed this behavior, for which the results are
28 the subject of a forthcoming publication [2].

29
30 We have added the following comment in the end of the Conclusion. On Page 5 Line 3, it now
31 reads "*Introducing more QWs in c-LEDs could further reduce QW carrier densities and quench
32 the efficiency droop since carrier delocalization and homogeneous injection are enabled in
33 multiple QWs by the lack of internal polarization and carrier effective mass reduction.*"

34
35 [1] I. Wildeson, "Progress and outlook for III-nitride blue, green and longer wavelength direct
36 emitters," in DOE SSL R&D Workshop, Nashville, TN, 2018.

37 [2] Y.-C. Tsai, C. Bayram, and J.-P. Leburton, J. Appl. Phys., 2022. (submitted)

1
2
3
4
5
6
7
8 **Response to Reviewer #2's Comments**
9

10 **General comments:**
11
12
13
14
15
16
17
18
19
20
21
22

23 *This work applies an interesting approach, a mixed semiclassical and quantum computational
24 method, to investigate the cause of efficiency droop in nitride-based LEDs. The work is clearly
25 written and its scope is also clear. Authors ascribe the QE droop to the presence of polarization
26 charges in hex. InGaN, and in fact they observe less droop for the cubic phase. This is a very well
27 known result, see e.g., Piprek in DOI=10.1007/s11082-011-9437-z, or Saguatti in
28 DOI=10.1109/TED.2012.2186579, even if many other mechanisms contribute to the QE droop.
29 Also the fact that the ABC-model overestimates the Auger effect is well known. Nevertheless, the
30 analysis in the present work compares several kind of nitride-based LEDs with different crystalline
31 phases, and a similar work is not present in literature. For this reason, I recommend it for the
32 publication, suggesting to include a wider literature analysis about well-known facts (e.g. the
33 known limitations of the ABC-model, and the also known role of the polarization charge).*

34
35 **A:** We thank the Referee for his/her positive and encouraging comments on our manuscript. As
36 stated in our manuscript, we conclude that the coexistence of strong internal polarization and large
37 hole effective mass induce carrier localization, poor electron-hole wavefunction overlap, large
38 carrier densities causing strong Auger recombination, and thus result in strong efficiency droop.
39 This explanation is different from the one reported by Piprek and Saguatti who suggest carrier
40 leakage (caused by strong internal polarization) is the cause of the efficiency droop. However,
41 their studies did not comment on the carrier densities and Auger recombination rate, which could
42 potentially result from a misinterpretation of the influence of internal polarization on the efficiency
43 droop.

44
45 For this reason, we have added a comment in the discussion of Fig. 3 and added the two references
46 suggested by the Referee as Refs. 22 and 23. On Page 4 Line 46 now reads “*It should be
47 emphasized that the efficiency droop reduction in non-polar h-LEDs that was previously attributed
48 to the decrease of carrier leakage from active region overlooks the interplay between internal
49 polarization and Auger recombination.[21], [22] Indeed, recent experiments suggest that the
50 efficiency droop reduction in non-polar h-LEDs is in fact due to carrier delocalization, (a situation
51 different than in polar h-LEDs) that results in stronger electron-hole wavefunction overlap, lower
52 QW carrier densities, and lower Auger recombination rates.[23]*”

53
54 We have added a short discussion on the ABC-model with an explicit statement on Page 4 Line
55 17, that now reads “*Despite the fact that the effective ambipolar Auger coefficient (C_a) in QWs is
56 calculated by multiplying the bulk C_a value by the squared electron-hole wavefunction overlap,[25]
57 prior studies have shown that disregarding this electron-hole wavefunction overlap would result
58 in an overestimation of the C_a value.[26] This overestimation is observed in the present study,
59 where we consider the influence of Auger electron-hole asymmetry ($C_n/C_p \neq 1$) on the efficiency
60 droop.*”

1
2
3 **Technical comments:**
45 **R2:** Just a minor technical point: please give some hint about the reason of the Auger peak in Fig.
6 1(d), left panel, since this is an important point. Why a peak is present? Authors claim that this is
7 due to the reduced wavefunction overlap, but I cannot figure out why.
89
10 **A:** We appreciate the Referee's positive and encouraging comments on the quality of our work.
11 The strong hole localization caused by the coexistence of internal polarization and large hole
12 effective mass shifts the peak hole density to higher values than the peak values in the electron
13 density. As a result, the *hhe* Auger recombination rate (determined by $C_{pp^2}n$) exhibits a higher
14 peak than the *eeh* Auger recombination rate peak (determined by C_nn^2p).
1516 We have revised the manuscript to clarify this issue. On Page 4 Line 13, it now reads "*It is seen*
17 *that the strong hole localization caused by the coexistence of strong internal polarization and*
18 *large hole effective mass in the h-LED (left panel) boosts the peak hole density and enhances the*
19 *hhe Auger recombination.*"
20
21
22
23
24
25
26
27
28
29
30
31
32
33
34
35
36
37
38
39
40
41
42
43
44
45
46
47
48
49
50
51
52
53
54
55
56
57
58
59
60

Response to Reviewer #3's Comments

General comments:

The authors argue that Auger/spontaneous recombination should be lower/higher in cubic InGaAlN. This is an interesting topic, but their logic is flawed because they use a simplistic model for Auger recombination ($Cn2p$ and $Cpn2$) and assume the Auger coefficient, C , is the same for both cubic and wurtzite GaN. The paper is too premature and requires a more rigorous calculation or measurement of Auger recombination in cubic InGaAlN. Details of the rejection to follow.

A: We are obviously disappointed by the Referee's recommendations that may have resulted from misreading the significance of our work. Below, we respond in details to all his technical comments.

Technical comments:

R.3.1: It is acceptable that the spontaneous emission is higher in cubic InAlGaN. I assume that they calculate the Auger recombination using C_{n2p} and C_{pn2} . Assuming C is the same for cubic and wurtzite is wrong. The reference used to justify doing this suggests that C could be even lower. However, that reference is for a band-to-band process that does not work even for wurtzite. Other physics needs to be included, such as a phonon-assisted process (<https://doi.org/10.1063/1.3570656> and <https://doi.org.prox.lib.ncsu.edu/10.1002/pssc.200880865> for example). It is unknown what including these types of processes does to cubic InAlGaN.

A: We respectfully disagree with the Referee on this issue for several reasons.

(1) The calculated Auger coefficients are subjected to great uncertainty owing to lack of experimental data on the high energy band structure. So, the calculated Auger coefficient in h-LEDs available nowadays relies on several assumptions. First, the calculations are limited to bulk band structures, where the Auger transitions among the subbands structures formed in quantum wells are ignored. Second, the strain effects and their effects on the subband structures and the Auger transitions are neglected. One of our prior studies in long-wavelength strained-layer quantum-well structures (doi:10.1109/3.375931) had shown that these two points are important to reproduce the measured Auger coefficient and had demonstrated the complexity of the calculation.

(2) For instance, in h-InGaN, indirect Auger recombination was proposed to fill the gap between the direct Auger coefficient and the measured Auger coefficient. Yet, the calculation results neither agree with each other nor match the measurements. For h-InGaN with a bandgap of 2.8 eV, for example, *Bertazzi et al* (doi: 10.1063/1.4733353) report an indirect Auger coefficient of $5.6 \times 10^{-32} \text{ cm}^6 \text{s}^{-1}$, *Kioupakis et al* (doi: 10.1063/1.3570656) report an indirect Auger coefficient of $1.8 \times 10^{-31} \text{ cm}^6 \text{s}^{-1}$, and interestingly, the same authors (*Kioupakis et al*) report another value of 5.1×10^{-31}

1
2
3 cm⁶s⁻¹ in doi: 10.1103/PhysRevB.92.035207. Despite all these theoretical efforts, the measured
4 value of 2.0×10^{-30} cm⁶s⁻¹ is still 4+ times larger than the calculated values. These considerations
5 suggest that by assuming the same (measured) Auger coefficient for h- and c-InGaN, one is less
6 likely to overestimate c-LED performances.
7

8 (3) The mechanism driving indirect Auger recombination is vaguely identified. *Kioupakis et al* in
9 doi: 10.1063/1.3570656 suggest that phonon-assisted Auger recombination is the major indirect
10 Auger mechanism, but, in doi: 10.1103/PhysRevB.92.035207, the later becomes alloy-assisted
11 Auger recombination. *Tan et al* (doi:10.1063/1.4978777) indicate interface roughness scattering
12 as the dominant indirect Auger mechanism in sub-3nm QWs. .
13

14 (4) The c-GaN Auger coefficient is overestimated if an ambipolar Auger coefficient of 2.0×10^{-30}
15 cm⁶s⁻¹ is assumed. By comparing the electronic structure of c-GaN with that of h-GaN, one can
16 see that c-GaN has significantly fewer energy states close to the conduction band minimum and
17 the valence band maximum. (doi:10.1038/s41598-019-43113-w and doi:10.1063/1.4829674) In
18 particular, the energy difference between the first and second conduction bands at the Γ point is >8
19 eV. (doi: 10.1063/1.3133359) These effects combined are expected to impede both direct and
20 indirect Auger transitions, leading to lower C_n and C_p with respect to h-GaN.
21

22 We have revised the manuscript and added one reference as Ref. 21. On Page 3 Line 3, it now
23 reads “*It should be pointed out that the C_n and C_p in c-LEDs have not yet been reported in the
24 literature. However, by comparing the electronic structure of c-GaN with that of h-GaN,[17], [21]
25 one can see that c-GaN has significantly fewer energy states close to the conduction band minimum
26 and the valence band maximum. In particular, the energy difference between the first and second
27 conduction bands at the Γ point is >8 eV.[17], [20] These effects in combined are expected to
28 impede both direct and indirect Auger transitions, leading to lower C_n and C_p with respect to h-
29 GaN.*”
30

31
32
33
34
35
36
37
38 R3.2: *A more rigorous calculation that includes overlap and matrix elements needs to be
39 performed to provide a meaningful Auger recombination (or coefficient) for cubic InAlGaN.
40 Alternatively, measurement of Auger recombination as has been done in wurtzite InAlGaN (see
41 http://dx.doi.org/10.1149/2.0372001JSS).*
42

43 A: We appreciate the Referee’s comment. However, the experimental Auger coefficients of c-
44 LEDs are unavailable. Alternatively, we have considered the uncertainties on C_n , C_p , and C_a
45 ($=C_n+C_p$) and their influences on the efficiency droop for both h-LEDs and c-LEDs in Fig. 4. It is
46 clear that c-LED efficiency droop is much immune to the C_n/C_p value and the increase of C_a , for
47 which the main statement: “*carrier localization caused by the coexistence of strong internal
48 polarization and large carrier effective mass leads to strong Auger recombination and, thus,
49 efficiency droop*” holds.
50

1
2
3
4 *R3.3: In=30% is much too high for a green LED in wurtzite InGaN. It is usually between 20-25%.*
5
6
7
8
9
10
11
12
13

A: According to the literature, InGaN QWs with a 30% indium mole fraction could have a peak emission wavelength at ~525 nm (doi: 10.1002/pssa.200880926), while theoretical studies report a range of 25–30% for the peak emission wavelength from 480–520 nm (doi:10.1103/PhysRevLett.116.027401). Since the efficiency droop increases with respect to the increased indium mole fraction, we choose the maximum indium mole fraction within this range as the worst-case scenario.
14
15
16
17
18
19
20
21
22
23
24
25
26
27
28
29
30
31
32
33
34
35
36
37
38
39
40
41
42
43
44
45
46
47
48
49
50
51
52
53
54
55
56
57
58
59
60